Sensors & Transducers, Vol. 226, Issue 10, October 2018, pp. 77-82

www.sensorsportal.com

Sensors & Transducers

Published by IFSA Publishing, S. L., 2018
http://www.sensorsportal.com

Autofocus in Two-Wavelength Contouring for Fast Inspection of Micro Parts

[1, 2] Mostafa AGOUR, [1] Claas FALLDORF and [1, 3] Ralf B. BERGMANN

[1] BIAS – Bremen Institute of Applied Beam Technology, Klagenfurter Straße 5, 28359 Bremen, Germany

[2] Aswan s, Faculty of Science, Department of Physics, 81528 Aswan, Egypt

[3] University of Bremen, Faculty 01: Physics and Electrical Engineering and MAPEX Center for Materials and Processes, 28359 Bremen, Germany

E-mail: agour@bias.de

Received: 25 June 2018 /Accepted: 31 August 2018 /Published: 31 October 2018

Abstract: We present a method for fast inspection of metallic micro parts. It is based on the combination of two-wavelength contouring and digital holographic microscopy (DHM). For fast evaluation, an autofocus algorithm to refocus the object digitally without the need for any external intervention is proposed. The method enhances the microscope objective's depth of focus compared with imaging techniques by standard microscopy. Compared to standard DHM, an object side telecentric objective is utilized to overcome irreversible depth distortions caused by standard microscope objectives. The method is demonstrated by reconstructing the three-dimensional shape of a metallic deep drawn micro cup. Experimental results confirm the improved depth of focus of DHM.

Keywords: Digital holographic microscopy, Holographic contouring, Shape and deformation measurement, Depth of focus, Micro deep drawing parts.

1. Introduction

Micro parts are commonly fabricated at a high production rate. The manufacturing in such a mass production process which contains prototyping and production has to be cost-effective. The cold drawing process is one of the cost-effective production processes and it produces up to several hundreds of micro parts per minute. Usually, micro parts should have defined shape and surface characteristics. These characteristics strongly depend on the production tools and steps used to manufacturing them [1].

In general, micro parts are subject to dimensional errors which lead to form deformation and surface defects such as dent, scratches, and fractures. Thus, quality inspection is an important task to improve and monitor the production process. For inspection, metrology techniques such as tactile, confocal microscope, white light interferometry [2], phase retrieval [3-5] and computational shear interferometry (CoSI) [6] were used. In regard to in-line inspection, such techniques are not suited since they are based on scanning and/or require a set of sequential measurements. In contrast to these methods, digital holography (DH) [7] offers fast measurements with resolution down to fractions of the wavelength of the illumination. DH offers a direct access to the phase difference of the coherent superposition of light diffracted from the test object and a separate reference beam. Thus, the optical path difference (OPD) of light diffracted by the test object which is directly correlated with its geometric and surface properties can be measured. However, phase ambiguities occur when the height difference between two points of a test

surface is larger than a quarter of the wavelength. Especially if the investigated surface is optically rough, the result of the evaluation becomes ambiguous and cannot be used to reconstruct the shape of the test object. One way to solve this problem is realized by recording two holograms to recover two phase distributions associated with two different wavelengths. This approach is referred to as two-wavelengths contouring technique [8-9]. The results of the two-wavelength measurement equal that of a single measurement with a much larger wavelength Λ which is often referred to as the synthetic wavelength. This relaxes the ambiguity problem to step heights of $\Lambda/4$.

Here we present a fast shape measurement method which can be used for in-line quality inspection of micro parts. The method is based on implementation of autofocus in holographic two wavelength contouring. The method enhances the depth of focus of the utilized DHM objective. For fast acquisition, holographic spatial frequency multiplexing is realized to capture the required two holograms in a single shot. The method is demonstrated by measuring the 3D form of a metallic micro cup.

2. Form Measurements by Means of Holographic Contouring

This technique consists of two main processes: the measurement which requires a holographic setup to capture the required hologram and an evaluation process to convert the measurement to a 3D form map. Since it is planned to investigate micro objects, digital holographic microscopy DHM is considered [8-9]. Fig. 1 shows a scheme of the utilized DHM [10].

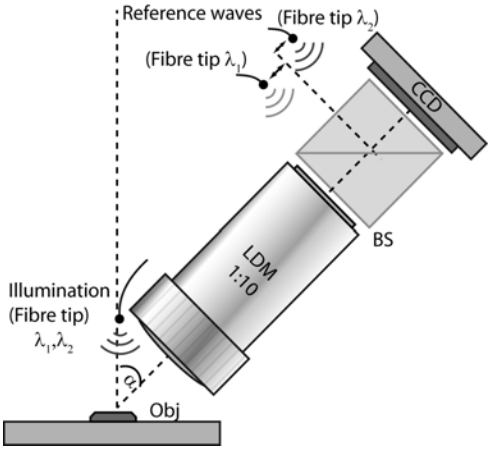

Fig. 1. A scheme of the used DHM setup: LDM refers to an object side telecentric long distance microscope objective having 10× magnification, a numerical aperture of NA= 0.21 and a working distance of 51 mm. Obj refers to the test object and BS is a 50:50 beam splitter.

The setup consists of a long distance microscope objective (LDM) with a 10× magnification, a numerical aperture (NA) of 0.21 and a working distance (WD) of 51 mm. The LDM is an object side telecentric objective. It is noted that the NA of the microscope objective limits the depth of field which is planned to be extended by means of digital refocusing in digital holograph. BS is a beam-splitter combining light diffracted from the surface under test and the reference wave resulting in a hologram for each wavelength across the camera plane. The holograms are then captured using a charge-coupled device (CCD) camera sensor located in the camera plane. It is noted that there exists an angle α between the observation and illumination direction.

However, technical objects' surfaces are optically rough, since the object surface commonly exhibits steps and peaks larger than quarter of the single wavelength. Thus, the evaluation process as a result of the measurement becomes ambiguous. Due to these phase ambiguities the surface form of the test object cannot be reconstructed from the measurement. Holographic two-wavelength contouring method can be used to solve this problem. In this approach, two complex amplitudes, $U_{\lambda 1}$ and $U_{\lambda 2}$, are retrieved from two measurements associated with two different wavelengths λ_1 and λ_2. In order to simultaneously record the two holograms associated with λ_1 and λ_2 in a single shot, three optical fiber splitter/coupler are used. The scheme for the realization of object illumination and reference beams is shown in Fig. 2.

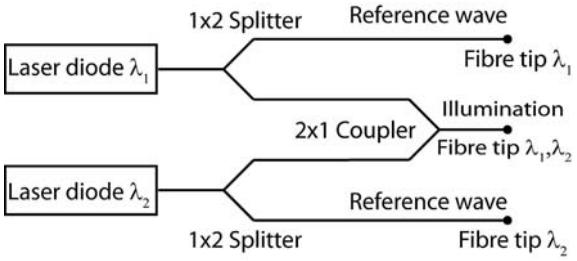

Fig. 2. Object and reference illumination scheme for the experimental setup. The scheme results in two reference waves and one illumination wave fiber tip, where light emitted from both laser diodes is mixed. This is realized using three 1×2 fiber splitter/coupler.

Each laser diode is coupled into a single mode fiber. Using a 1×2 fiber splitter, the input of each is divided into two outputs. Two of these outputs are used for illuminating the test object from one direction by combining them using a 1×2 coupler with an illuminating angle of $\propto = 22°$. The other two outputs are used as reference waves. The positions of the two reference waves are shifted from the center of the optical axis by different shifts of $\Delta x_n = (\Delta x_{ni}, \Delta x_{nj})$. Accordingly, the interference of the spherical wave arising from the field curvature of the objective and the shifted reference point source generates linear fringes, i.e. a linear phase ramp [4]. Since the two reference waves are shifted with a different amount of

shift, the corresponding holograms generated across the recording plane are modulated by different phase ramps $G_{\lambda n}$ which are given by

$$G_{\lambda n}(\mathrm{x}) = \exp[\mathrm{i}2\pi\Delta \mathrm{x}_\mathrm{n} \cdot \mathrm{x}] \quad (1)$$

Here, x = (x_i, x_j) represents a two dimensions vector at the recording, i.e., hologram, plane. The intensity distribution of the hologram generated at the camera plane which is captured using the CCD sensor can be written as

$$I_{\lambda 1,\lambda 2}(\mathrm{x}) = A(\mathrm{x}) + B(\mathrm{x}) + C(\mathrm{x}), \quad (2)$$

where A(x) represents the incoherent summation of the intensities of the interfering wave fields i.e. dc-term and B(x) and C(x) are given by

$$B(\mathrm{x}) = \sum_{n=1}^{2} \left(U_{O_{\lambda n}}(\mathrm{x}) \cdot U^*_{R_{\lambda n}}(\mathrm{x}) \cdot G_{\lambda n}(\mathrm{x})\right), \quad (3)$$

$$C(\mathrm{x}) = \sum_{n=1}^{2} \left(U^*_{O_{\lambda n}}(\mathrm{x}) \cdot U_{R_{\lambda n}}(\mathrm{x}) \cdot G^*_{\lambda n}(\mathrm{x})\right) \quad (4)$$

Here, $U_{O_{\lambda n}}$ and $U_{R_{\lambda n}}$ denote the object and reference wave fields, respectively, and * referrers to the complex conjugate. According to Eq. (3) and Eq. (4), the phase ramps introduce different spatial carriers to the holograms and thus they are laterally separated at the frequency domain obtained by applying a fast Fourier transform. A scheme of the expected spectrum of a single hologram containing object's information from the two simultaneous illuminations is shown in Fig. 3. Here +1, −1, and the dc-term refer to the diffraction orders, i.e., the plus and the minus first diffraction orders and the dc-term of an intensity hologram. The diffraction orders are laterally separated confirming that there was no crosstalk between the two generated holograms.

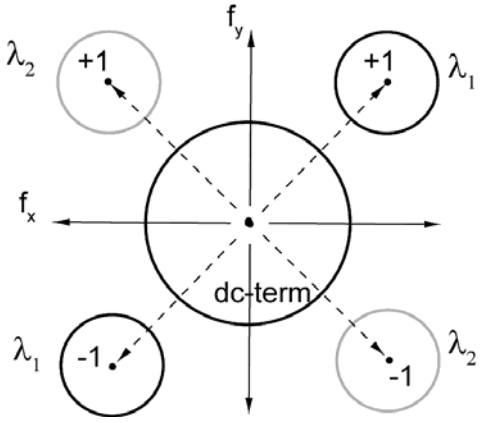

Fig. 3. Schematic representation of the expected spectrum of a single hologram, where +1, −1, and the dc-term refer to the diffraction orders and f_x and f_y represents the spatial frequencies in x and y directions.

In the following section, recovering the phase information from the recorded holograms will be discussed.

3. Recovering the Phase Information Form the Recorded Hologram

The adaptive spatial carrier frequency method [11-13] is applied in order to retrieve two complex amplitudes corresponding to λ_1 and λ_2 from the recorded intensity hologram. This is done by implementing the following steps:

1) Applying the fast Fourier transform on the recorded intensity hologram.

2) The spatial frequencies which are corresponding to the minus first diffraction order recorded for λ_1 is selected and all other frequencies are filtered out including the dc-term.

3) The selected frequencies area is translated to the center of the spectrum.

4) To obtain the complex amplitude $U_{\lambda 1}$ at the hologram plane an inverse fast Fourier transform is applied.

5) Steps 2 to 4 are repeated for the minus first diffraction order related to λ_2.

Thus, two complex amplitudes, $U_{\lambda 1}$ and $U_{\lambda 2}$, are retrieved from a one hologram recorded for the two wavelengths λ_1 and λ_2.

4. Holographic Contouring

From the two complex amplitudes across the hologram plane, $U_{\lambda 1}$ and $U_{\lambda 2}$, which are retrieved for the two different wavelengths λ_1 and λ_2, the corresponding complex amplitudes across the object plane, $U_{O_{\lambda 1}}$ and $U_{O_{\lambda 2}}$, are numerically determined. By tacking the argument of $U_{O_{\lambda 1}}$ and $U_{O_{\lambda 2}}$ the phase distributions at the object plane are calculated. Subtracting the two retrieved phase distributions across the object plane gives the phase difference $\Delta\phi$ across the object plane. From $\Delta\phi$ the 3D height map z_p of the test object is directly calculated utilizing [14]

$$\Delta\phi(\mathrm{x}) = -\frac{2\pi}{\Lambda} z_p(1 + \cos\alpha) \quad (5)$$

Here, α is the angle between the observation and illumination direction and Λ is referred to as the synthetic wavelength which is given by

$$\Lambda = \frac{\lambda_1\lambda_2}{|\lambda_2 - \lambda_1|} \quad (6)$$

The resulting phase difference distribution map given by $\Delta\phi$ equivalents a single measurement with Λ. This map contains fringes and it is referred to as the phase contouring map.

5. Autofocus for Form Measurements

Since the microscope objective of the DHM has a limited depth of focus, sharp contouring fringes appear only within the microscope objective's depth of field which is limited to a few microns. In this section, an autofocus method is used to enable the reconstruction of a complete sharp contouring map which covers the micro part under test. This phase map is used then to retrieve the 3D form of the test object. The approach is based on using an error metric which is calculated based on the standard deviation of the phase difference residuals. The error metric is given by [15]

$$\mathrm{E} = \sum_{x \in A} |\nabla \phi_{Res}|^2, \qquad (7)$$

where $\nabla\phi_{\mathrm{Res}}$ is the phase difference residual and is determined by subtracting the phase recovered from each measurement and its low pass filtered phase distribution. ∇ is the nabla operator which is applied in two dimensions. Hence, the minimum total variance of ϕ_{Res} is used to define where the object is in focus. The implementation of the whole process is summarized in the following steps:

1) Recover the complex amplitude across a certain plane in the object space for each wavelength using the spatial phase shifting approach. Thus, two phase distributions are obtained at the regarded plane as shown by the simulated results in Fig. 4(a, b).

2) Numerical propagation of the recovered complex amplitudes in various planes to cover the whole test object. The result of phase difference between the recovered phase distributions across the same plane gives a contouring map, as shown in Fig. 3(c), with sharp fringes only where the object is in focus. Propagating the recovered wave field U_{z_n} numerically from the plane located at z_n to the plane at z_m can be described by convolution of the wave field U_{z_n} with a linear shift invariant impulse response h_z [16] by:

$$U_{z_m}(\mathrm{x}) = \left(U_{z_n} \otimes h_z\right)(\mathrm{x}) \qquad (8)$$

Here, U_{z_m} denotes the complex amplitude of the propagated wave field and the index z refers to the propagation distance. The transfer function of propagation is a phasor with unit amplitude given by

$$h_z(\mathrm{x}-\mathrm{u}) = -\frac{i}{\lambda}\frac{\exp(ik|r|)}{|r|}\cos(\mathrm{z},\mathrm{r}), \qquad (9)$$

where k is the wave number and r = (x-u, z) is a vector connecting two positions of the respective propagation planes.

3) The focus region is indicated by monitoring the error metric, Eq. (7), and masking only the area where the object is in focus.

4) Step 3 is repeated for all object layers defining the area where the object is in focus.

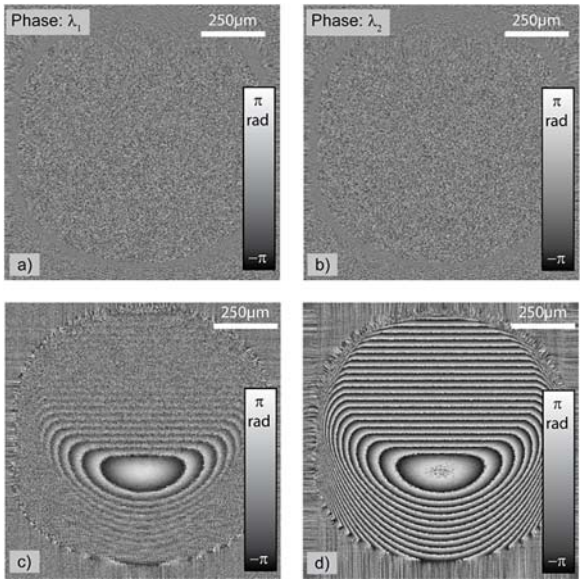

Fig. 4. Simulation of light diffracted from a metallic micro cup with 1 mm diameter, 0.5 mm height and a surface roughness of 5 µm. In a) and b) two phase distributions for λ = 637 nm and λ = 642 nm are shown. In c) the phase difference of a) and b) is given, with sharp fringes across the area where the object is in focus. d) shows the contouring phase map constructed by numerical propagation through various layers in the object space. The map shows sharp fringes across the entire object.

5) At this step all areas found to be in focus are stitched together to construct a contouring map where sharp fringes covering the entire object as shown in Fig. 4(d).

The resulting contouring phase map is then unwrapped. The values of the unwrapped phase are substituted in Eq. (5) to reconstruct a 3D height map of the test object. The 3D map could be used, e.g., to inspect the geometry of the test object.

6. Experimental Results

Fig. 5 shows the test object which is a metallic micro cold formed cup having a radius of ca. 500 µm and depth of ca. 500 µm.

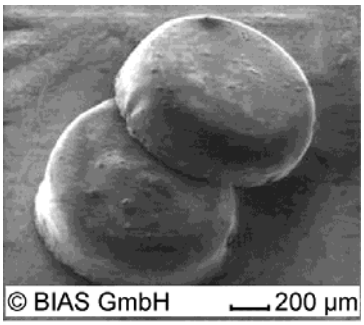

Fig. 5. Scanning electron micrograph of a metallic cold formed micro-cup [14].

The object and reference illumination scheme for the experimental setup is constructed based on the scheme given in Fig. 2. To this purpose, two laser diodes $\lambda_1 = 636.55$ nm and $\lambda_2 = 642.10$ nm and three 1×2 fiber splitters and couplers are used. Hence, according to Eq. (6), a synthetic wavelength of $\Lambda = 73.64$ µm is utilized for the evaluation process.

Fig.6a shows an example of a captured hologram. And Fig. 6 (b) shows its spectrum which contains all information required for implementing the contouring approach. It is noted here, that there is no cross talk between the two different holograms which are recorded in a single shot camera image. Each object's information related to certain wavelength is shifted according to an exact position.

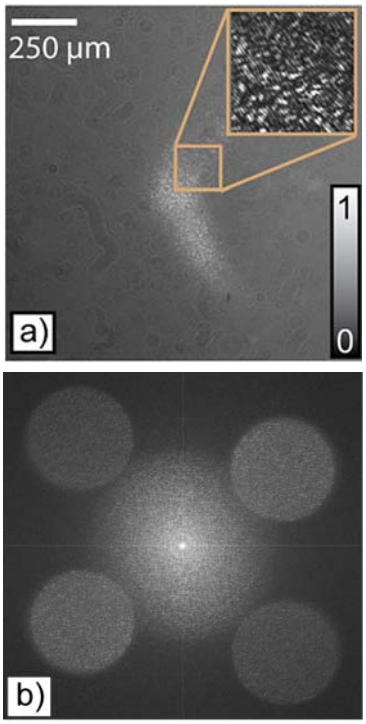

Fig. 6. Image a) shows a single hologram which contains object information for the simultaneous illumination of two wavelengths and b) shows its spectrum.

As seen from Fig. 7(a, b), the contouring fringes are only sharp for the plane which is in-focus due to the limited depth of focus of the utilized microscope objective. Areas out of focus are corrupted by speckle decorrelation, as predicted by the simulation results shown in Fig. 4.

To obtain a sharp contouring map across the whole object, the recovered object wave is numerically propagated throughout all objects planes using Eq. (8). The autofocus algorithm is implemented by scanning within small windows throughout all propagated planes to define where the object is in focus minimizing Eq. (7). Accordingly, different areas where the object is in-focus are found and stitched together forming the sharp amplitude image of micro-cup, Fig. 7 (c), and the contouring map, see Fig. 7(d). For fast evaluation, an automated process was proposed and implemented within a graphics processing unit (GPU). For this a GTX 1080 graphic card having 8 GB Ram is used. Using this unit the evaluation process is done in less than one second.

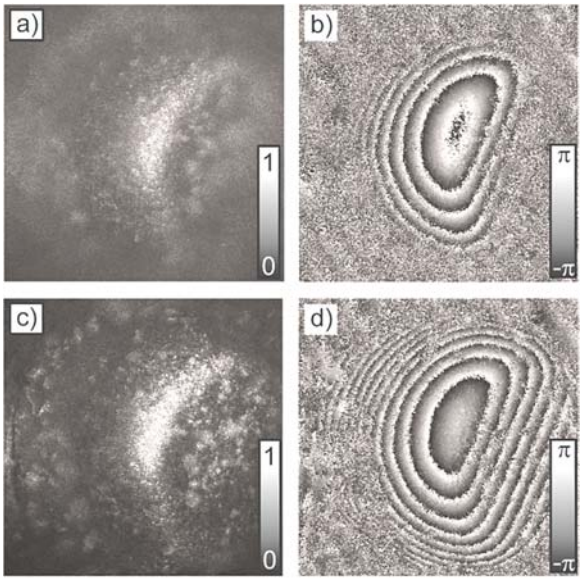

Fig. 7. Reconstructed intensities which represent a sharp image of the micro cup under test at one plane a) and across the whole object after the digital extending DHM depth of focus b) are shown. And b) and d) show the corresponding phase difference. Image size is 2200 × 2200 pixels with a pixel pitch of 4.54 µm.

To reconstruct the 3D form of the measured micro-cup, the phase contouring map presented in Fig. 7(d) is unwrapped using Goldstein phase unwrapping approach [17]. By substituting the unwrapped phase values in Eq. (5), the 3D height map which is presented in Fig. 8 is obtained.

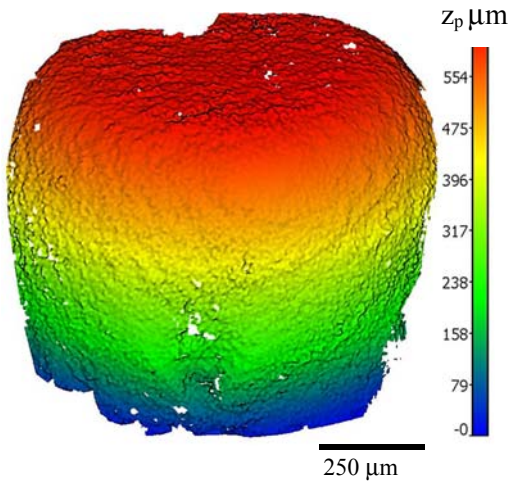

Fig. 8. 3D form of a metallic micro-cup reconstructed by substituting the unwrapped phase values of the phase contouring map into Eq. (5).

7. Conclusions

We present a fast approach for geometrical inspection of cold formed micro parts. It uses two-wavelength holographic contouring in digital holographic microscopy (DHM). Using autofocus, the depth of field of the DHM is extended. The autofocus approach defines the plane where the object is in focus by estimating the standard deviation of the contouring phase map $\Delta\phi_{Res}$ which is relatively high within areas where the object is out of focus because of the speckle decorrelation. For fast evaluation, the method is implemented in a GPU. The method is demonstrated by reconstructing the 3D geometrical shape of a metallic cold formed micro-cup.

Acknowledgements

The authors gratefully acknowledge the financial support by the Deutsche Forschungsgemeinschaft (DFG, German Research Foundation) for Subproject B5 "Safe processes" within the Collaborative Research Center "SFB 747 - Micro cold Forming".

References

[1]. C. von Kopylow, R. B. Bergmann, Optical Metrology, in Micro Metal Forming, *Springer,* Heidelberg, 2013, pp. 392–404.

[2]. J. C. Wyant, White light interferometry, in Holography, *SPIE,* Vol. 4737, 2002, pp. 98-108.

[3]. M. Agour, P. Huke, C. Kopylow, C. Falldorf, Shape measurement by means of phase retrieval using a spatial light modulator, in *Proceedings of the International Conference on Advanced Phase Measurement Methods in Optics and Imaging, AIP,* Vol. 1236, 2010, pp. 265-270.

[4]. C. Falldorf, M. Agour, C. Von Kopylow, R. B. Bergmann, Phase retrieval for optical inspection of technical components, *J. Optics*, Vol. 14, Issue 6, 2012, pp. 065701.

[5]. M. Agour, C. Falldorf, R. B. Bergmann, Investigation of composite materials using SLM-based phase retrieval, *Opt. Letters*, Vol. 38, Issue 13, 2013, pp. 2203–2205.

[6]. C. Falldorf, M. Agour, R. B. Bergmann, Digital holography and quantitative phase contrast imaging using computational shear interferometry, *Opt. Engineering*, Vol. 54, Issue 2, 2015, pp. 024110.

[7]. U. Schnars, W. Jüptner, Direct recording of holograms by a CCD target and numerical reconstruction, *Appl. Optics*, Vol. 33, Issue 2, 1994, pp. 179–181.

[8]. M. Agour, R. Klattenhoff, C. Falldorf, R. B. Bergmann, Spatial multiplexing digital holography for speckle noise reduction in single-shot holographic two-wavelength contouring, *Opt. Engineering*, Vol. 56, Issue 12, 2017, p. 124101.

[9]. M. Agour, R. Klattenhoff, C. Falldorf, R. B. Bergmann, Speckle noise reduction in single-shot holographic two-wavelength contouring, in *Proceedings of the SPIE*, Vol. 10233, 2017, p. 102330R.

[10]. M. Agour, C. Falldorf, R. B. Bergmann, Extended Depth of Focus using Autofocus in two wavelength contouring for fast inspection of micro parts, in *Proceedings of the 1st International Conference on Optics, Photonics and Lasers (OPAL'18)*, Barcelona, Spain, 9-11 May 2018, pp. 205-208.

[11]. M. Takeda, H. Yamamoto, Fourier-transform speckle profilometry: three-dimensional shape measurements of diffuse objects with large height steps and/or spatially isolated surfaces, *Appl. Optics*, Vol. 33, Issue 34, 1994, pp. 7829–7837.

[12]. M. Agour, K. El-Farahaty, E. Seisa, E. Omar, T. Sokkar, Single-shot digital holography for fast measuring optical properties of fibers, *Appl. Optics*, Vol. 54, Issue 28, 2015, pp. E188–E195.

[13]. T. Sokkar, K. El-Farahaty, M. El-Bakary, E. Omar, M. Agour. A. Hamza, Adaptive spatial carrier frequency method for fast monitoring optical properties of fibres, *Appl. Phys. B*, Vol. 122, Issue 5, 2016, pp. 1–14.

[14]. N. Wang, C. von Kopylow, C. Falldorf, Rapid shape measurement of micro deep drawing parts by means of digital holographic contouring, in *Proceedings of the 36th MATADOR Conference,* eds.: S. Hinduja, L. Li, *Springer Verlag*, London, 2010, pp. 45–48.

[15]. C. Falldorf, S. H. von Luepke, C. von Kopylow, R. B. Bergmann, Reduction of speckle noise in multiwavelength contouring, *Appl. Optics*, Vol. 51, Issue 34, 2012, pp. 8211-8215.

[16]. M. Agour, C. Falldorf, R. B. Bergmann, Spatial multiplexing and autofocus in holographic contouring for inspection of micro-parts, *Optics Express,* Vol. 26, Issue 22, 2018, pp. 28576-28588.

[17]. G. C. Sherman, Application of the convolution theorem to Rayleigh's integral formulas, *J. Opt. Soc. Am.*, Vol. 57, Issue 4, 1967, pp. 546–547.

[18]. R. M. Goldstein, H. A. Zebken, C. L. Werner, Satellite radar interferometry: Two-dimensional phase unwrapping, *Radio Sci.*, Vol. 23, Issue 4, 1988, pp. 713-720.